Journal of Visualized Experiments

Quantifying tissue-specific proteostatic decline in Caenorhabditis elegans

--Manuscript Draft--

Article Type:	Invited Methods Collection - JoVE Produced Video
Manuscript Number:	JoVE61100R2
Full Title:	Quantifying tissue-specific proteostatic decline in Caenorhabditis elegans
Keywords:	Proteostasis; polyglutamine; polyQ::YPC; C. elegans; Aging; biomarker; protein homeostasis; genetic analysis; functional genomics
Corresponding Author:	Andrew Samuelson Univertsity of Rochester Medical Center Rochester, NY UNITED STATES
Corresponding Author's Institution:	Univertsity of Rochester Medical Center
Corresponding Author E-Mail:	andrew_samuelson@urmc.rochester.edu
Order of Authors:	Maria I. Lazaro-Pena
	Adam B. Cornwell
	Andrew Samuelson
Additional Information:	
Question	**Response**
Please indicate whether this article will be Standard Access or Open Access.	Standard Access (US$2,400)
Please indicate the **city, state/province, and country** where this article will be **filmed**. Please do not use abbreviations.	Rochester, NY, Monroe

TITLE:

Quantifying Tissue-Specific Proteostatic Decline in *Caenorhabditis elegans*

AUTHORS AND AFFILIATIONS:

Maria I. Lazaro-Pena, Adam B. Cornwell, Andrew V. Samuelson

Department of Biomedical Genetics, University of Rochester Medical Center, Rochester, New York, USA

María I. Lázaro-Peña
maria_lazaro-pena@urmc.rochester.edu

Adam B. Cornwell
adam_cornwell@urmc.rochester.edu

Corresponding author:
Andrew V. Anderson
andrew_samuelson@urmc.rochester.edu

KEYWORDS:

proteostasis, polyglutamine, *polyQ::YPC, C. elegans*, aging, biomarker, protein homeostasis, genetic analysis, functional genomics

SUMMARY:

Proteostatic decline is a hallmark of aging, facilitating the onset of neurodegenerative diseases. We outline a protocol to quantifiably measure proteostasis in two different *Caenorhabditis elegans* tissues through heterologous expression of polyglutamine repeats fused to a fluorescent reporter. This model allows rapid in vivo genetic analysis of proteostasis.

ABSTRACT:

The ability to maintain proper function and folding of the proteome (protein homeostasis) declines during normal aging, facilitating the onset of a growing number of age-associated diseases. For instance, proteins with polyglutamine expansions are prone to aggregation, as exemplified with the huntingtin protein and concomitant onset of Huntington's disease. The age-associated deterioration of the proteome has been widely studied through the use of transgenic *Caenorhabditis elegans* expressing polyQ repeats fused to a yellow fluorescent protein (YFP). This *polyQ::YFP* transgenic animal model facilitates the direct quantification of the age-associated decline of the proteome through imaging the progressive formation of fluorescent foci (i.e., protein aggregates) and subsequent onset of locomotion defects that develop as a result of the collapse of the proteome. Further, the expression of the *polyQ::YFP* transgene can be driven by tissue-specific promoters, allowing the assessment of proteostasis across tissues in the context of an intact multicellular organism. This model is highly amenable to genetic analysis, thus providing an approach to quantify aging that is complementary to lifespan assays. We describe how to accurately measure *polyQ::YFP* foci formation within either neurons or body wall muscle

during aging, and the subsequent onset of behavioral defects. Next, we highlight how these approaches can be adapted for higher throughput, and potential future applications using other emerging strategies for *C. elegans* genetic analysis.

INTRODUCTION

Protein homeostasis (proteostasis) is defined as the cellular ability to maintain proper function and folding of the proteome. The inherent challenge to proteostasis is ensuring all proteins are properly folded and maintained in a native conformation, which is further amplified by the varied nature of protein size, amino acid composition, structural conformation, stability, turnover, expression, sub-cellular compartmentalization, and modifications[1]. Proteostasis is maintained through the coordinated action of a large proteostatic network, consisting of approximately 2000 unique proteins, which regulate proper synthesis, folding, trafficking, and degradation within the proteome[2,3]. The workhorse components of the proteostatic network are nine major families of molecular chaperones[4]. Every tissue and cell type preferentially utilizes specific subsets of molecular chaperones, presumably in alignment with the differing demands of distinct proteomes[5].

One hallmark of normal organismal aging is the progressive decline and collapse of cellular proteostasis, which is thought to be an underlying basis for the onset and progression of a growing number of age-associated diseases. For instance, Alzheimer's disease, Parkinson's disease, Huntington's disease, and Amyotrophic Lateral Sclerosis (ALS) share a common characteristic: in each case manifestation of neurodegeneration is driven by genetic alterations that predisposes a mutant protein to aggregation (amyloid-β/Tau, α-synuclein, HTT, FUS/TBD-43/SOD-1, respectively)[6-10]. During aging, the integrity and inducibility of the proteostatic network declines, which results in the accumulation of proteotoxic aggregates that result in cellular dysfunction and neurodegeneration. Of note, protein conformational diseases are not unique to neurons, and occur across multiple tissues, as highlighted by type II diabetes, multiple myeloma, and cystic fibrosis[11-14]. Therefore, elucidating mechanisms capable of preserving proteostasis will facilitate the development of targeted interventions for the treatment of disease and to promote healthy aging.

The small soil nematode *Caenorhabditis elegans* (*C. elegans*) has been instrumental in discovering genes and elucidating pathways that alter proteostasis. Many components of the proteostatic network and the signal transduction pathways that regulate proteostasis are evolutionarily conserved. Furthermore, *C. elegans* has reduced complexity and redundancy relative to vertebrate systems, making it more amenable to genetic analysis and gene discovery. Additional advantages of *C. elegans* that have led to it being widely used as a model system to study proteostasis include: powerful genetic and functional genomics, a short life cycle (3 days) and lifespan (3 weeks), a compact and well-annotated genome, the availability of a wide assortment of genetic mutants, and the ease of visualizing tissue-specific changes in cell biology using fluorescent reporters.

The progressive decay of proteostasis during aging can be easily quantified in *C. elegans.* The Morimoto laboratory first demonstrated that a polyglutamine expansion fused to yellow

fluorescent protein (*polyQ::YFP*) could be used to quantify proteostatic decline in *C. elegans* during aging[15-18]. YFP fusions to 35 glutamine repeats or more result in an age-associated formation of fluorescent foci along with signs of cellular pathology. Of note, this range of glutamine expansion mirrors the length of the polyglutamine tract of the Huntingtin protein at which Huntington's Disease pathology begins to be observed in humans (typically >35 CAG repeats)[19]. Strains with expression of *polyQ::YFP* within muscle, intestinal, or neuronal cells have been utilized to confirm that the age-associated decline of proteostasis occurs across different cell and tissue types. Muscle-specific *polyQ::YFP* expression (i.e., *unc-54p::Q35::YFP*) has been the most widely used tissue-specific reporter, as accumulating fluorescent foci are easy to quantify over the first few days of adulthood using a simple fluorescent dissecting microscope (**Figure 1A-1B**). Additionally, animals become paralyzed during mid-life, as the proteome within the muscle collapses due to the proteotoxic effect of the reporter (**Figure 1C**). Similarly, the age-associated decline in neuronal proteostasis can be followed (*rgef-1p::Q40::YFP*) by directly quantifying foci/aggregate formation and age-associated declines in coordinated body-bends after placing animals into liquid (**Figure 2**).

Here, we present a detailed protocol on how to measure the age-dependent progression of protein aggregate accumulation and the associated proteotoxicity induced by the expression of polyglutamine repeats within neuronal and muscle tissue in *C. elegans*. We provide examples of typical results generated using these strains and methods. Further, we show how we have utilized these methods to study transcriptional regulation of the proteostatic network. We discuss additional ways these reporters can be easily integrated with other existing reagents or adapted for larger screens.

PROTOCOL:

1. Preparation of reagents

1.1. Select genes of interest to be inactivated via feeding-based RNAi. Purchase stocks of HT115 *E. coli* containing the RNAi clone of interest [20]. Alternatively, subclone the cDNA of the gene of interest into the multicloning site of the L4440 plasmid.

NOTE: To prevent degradation of dsRNA within the bacteria, use the HT115 strain. This is an RNase III-deficient *E. coli* strain with IPTG-inducible T7 polymerase activity. For proteostasis studies that do not use feeding-based RNAi, either HT115 or OP50 *E. coli* on standard NGM plates can be used.

1.2. Prepare 5 x 6 cm plates per test condition. For experiments using RNAi, induce dsRNA production in transformed HT115 *E. coli*. For studies without RNAi, OP50 *E. coli* on standard NGM plates can be used (See **Supplemental File 1** for standard NGM and RNAi plate recipes).

NOTE**:** RNAi plates can be stored at 4 °C for several months before seeding with bacteria.

1.3. Grow cultures of *E. coli* overnight (16-20 h) at 37 °C in a shaking incubator at 220 rpm. Grow HT115 *E. coli* in Luria Broth (LB) with ampicillin (50 μg/mL).

NOTE: Standard OP50 *E. coli* is not antibiotic resistant, but streptomycin resistant variants are also available.

1.3.1. Concentrate bacteria by centrifugation at 2,400 x *g* for 15-20 min in a benchtop centrifuge, aspirate the supernatant, and re-suspend the pellet in 1/10th the starting volume (i.e., 10x concentration) of LB with ampicillin for HT115, or LB without ampicillin for standard OP50.

1.3.2. Aliquot 200 μL of concentrated 10x bacteria to each plate (3-4 replicates per test condition, with 2 extra backup plates, to be used in the event of contamination).

1.3.3. Allow open plates to dry in a clean environment such as a laminar flow bench until all liquid has been absorbed or allow covered plates to dry on a lab bench overnight.

1.4. For seeded RNAi plates dried in a hood, store dried plates within a worm box overnight (up to 24 hours) at room temperature. After 1 day at RT, plates can be stored at 4 °C for up to 2 weeks in a sealed bag (to prevent plates from drying out). Before use, allow plates stored at 4 °C to return to room temperature within the zip-lock bag to prevent condensation from introducing airborne fungal contaminates.

1.4.1. When using feeding-based RNAi, leave seeded HT115 bacteria on RNAi plates at room temperature for at least 12 hours prior to adding *C. elegans.* RNAi plates contain IPTG, which induces dsRNA production. Alternatively, IPTG can be added to the liquid cultures at the end of step 1.3.1, 2 hours prior to seeding.

1.4.2. Avoid long-term storage of seeded HT115 at room temperature (greater than a few days) to avoid cracking of the agar that will cause *C. elegans* to burrow into agar.

2. Synchronization of *C. elegans*

2.1. Choose whether to synchronize *C. elegans* by either alkaline hypochlorite treatment of gravid adults or egg lay.

2.1.1. For hypochlorite treatment, wash gravid hermaphrodites 2 times with M9 buffer, then resuspend in a 5 mL hypochlorite solution (3.25 mL of hypochlorite solution, 1 mL of M9 buffer and 0.75 mL of 5 M NaOH) for 5 min, shaking resuspended animals every minute. After 5 min, spin down animals and wash 3 times with M9 buffer.

2.1.2. For egg lay synchronization, place 20 gravid hermaphrodites on a plate with food and let them lay eggs for a period of 4 h. After 4 h, remove the hermaphrodites and keep the plate containing synchronized eggs.

NOTE: Hypochlorite treatment has been posited to affect proteostasis[21].

2.1.3. Freeze and store leftover L1 animals in liquid nitrogen or a -80 °C freezer. In this way, a sample of each strain at the time of the experimental setup is preserved, creating a valuable resource for future studies and improving reproducibility.

NOTE: See **Supplemental File 1** for hypochlorite and M9 solution recipes.

2.2. Synchronize animals by hypochlorite treatment of gravid adult animals to promote the release of embryos[22].

2.2.1. After hypochlorite treatment, allow embryos to hatch overnight in 3 mL of M9 solution with rotation at 20 °C.

2.2.2. Calculate the density of L1 animals (or alternatively, embryos) per µL by dropping 10 µL of L1 solution 3x onto a 6 cm plate and counting the number of L1 animals to calculate the average number of L1 animals per µL. L1 animals will settle over time. Therefore, periodically mix L1 solutions to avoid settling.

2.2.3. Seed 50 L1 animals per plate, count and record the number seeded, and move plates to a 20 °C incubator. It is important to know the actual number of animals on each plate at the start of the assay.

NOTE: Synchronizing L1 animals by overnight hatching in M9 is routinely used as it minimizes developmental heterogeneity after placing animals onto food. However, synchronization occurs through developmental arrest in response to starvation cues, which for some studies should be avoided (see [23] for additional discussion). As an alternative, roughly synchronized animals can be obtained through an egg-lay, see 2.2.

2.3. To synchronize animals via egg lay, place 5-10 young gravid adult animals (day 1 of adulthood) onto each plate for 4-6 hours, and allow them to lay eggs until there are approximately 50 eggs per plate.

NOTE: The gravid adult animals should be synchronized at the first day of adulthood. Older animals may lay eggs that have been retained in the uterus, causing the release of eggs that are in a more advanced developmental stage.

2.3.1. Remove all gravid adults and move plates with eggs to a 20 °C incubator.

3. Progeny production

NOTE: Steps must be taken to either prevent progeny production or to separate the synchronized starting population from their progeny. Preventing progeny production can be achieved chemically with addition of 5-Fluoro-2'-deoxyuridine (FUdR) to plates, which is described here.

Some studies have reported that FUdR can alter proteostasis[24,25]. Alternative approaches to prevent progeny production are discussed below.

3.1. Make a 1000x stock solution of FUdR by dissolving 1 g of FUdR into 10 mL of ultrapure H_2O. Filter sterilize stock FUdR with a 0.2 μm filter and a 10 mL syringe. Aliquot 1 mL of stock into a sterile 1.5 mL tube. Freeze and store at -20 °C.

3.2. Grow animals at 20 °C until the L4 stage. N2 animals raised from synchronized L1s from hypochlorite treatment require approximately 40 hours of growth at 20 °C to reach L4. Growth rates for other strains should be empirically tested prior to experimentation. For details on how to accurately stage *C. elegans* see[26].

3.2.1. To each 6 cm plate with L4 animals, add 50 μL of 160x FUdR. It is critical to add FUdR at the L4 stage.

3.3. Return plates to a worm box and put the box in a zip-lock bag. Return to appropriate incubator.

4. Measuring the decline in proteostasis in muscle tissue by using polyglutamine-expressing animals

NOTE: Two methods can be used to identify proteostasis decline in muscle cells: imaging the formation of protein aggregates during aging (4.1) and measuring the proteotoxicity these aggregates cause with age through the onset of paralysis (4.2).

4.1. Imaging polyglutamine aggregate formation in the muscle during aging

NOTE: The age-dependent progression of protein aggregation in the muscle cells is imaged using polyglutamine (polyQ) repeats fused to a yellow fluorescent protein (YFP). This protocol outlines use of strain AM140 *rmIs132[unc-54p::G35::YFP]*, but other polyglutamine variant strains can also be used. The *polyQ::YFP* transgene is expressed in the muscle using the *unc-54* muscle-specific promoter. Synchronized *unc-54p::polyQ::YFP* expressing animals are visualized at Day 1, 2, 3 and 4 of adulthood. To visualize *unc-54p::polyQ::YFP* aggregates, use a compound microscope equipped for fluorescence or a fluorescent dissecting microscope. AM140 is available from the Caenorhabditis Genetics Center (CGC) at: https://cgc.umn.edu/strain/AM140.

4.1.1. On imaging days (Day 1, 2, 3 and 4 of adulthood), pick 20 animals and mount on a microscope slide setup with a 3% agarose pad and a 5 μL drop of 10 mM sodium azide (diluted in M9 buffer).

4.1.2. After all worms are immobilized by sodium azide (~ 5 minutes), image the whole bodies of the animals using a 10x magnification lens (**Figure 1A**). For imaging, use a FITC filter and the same exposure for every animal. Discard slides after imaging.

NOTE: Alternatively, YFP foci can also be quantified directly on plates, but movement must be inhibited by applying a stream of carbon dioxide onto the plate while scoring. This alternative method is most appropriate when screening a large number of conditions (see discussion for more details).

4.1.3. After acquisition of images, count the number of foci in the body wall muscles of the whole animal. Foci are brighter punctuated signals that can be differentiated from the dimmer soluble signal in the background.

4.1.4. Plot the progression of YFP foci accumulation from days 1, 2, 3 and 4. Plot an XY graph where X represents days of adulthood and Y represents number of *unc-54p::polyQ::YFP* foci (**Figure 1B**). The number of foci in the experimental condition (e.g., gene downregulation or overexpression) is compared to control animals. Perform statistical analysis between the groups at each time point observed for each trial.

4.1.4.1. When comparing foci counts for only two conditions, perform an independent sample t-test at each time point.

4.1.4.2. When comparing foci counts for more than two conditions, perform an omnibus one-way ANOVA analysis for each time point, including the data for all the conditions at that time point. If the omnibus ANOVA yields a significant p-value (i.e., $p < 0.005$), perform a *post-hoc* analysis with pairwise independent sample t-tests to determine the specific conditions between which a significant difference in foci was detected (e.g., for groups A, B, and C compare A & B, A & C, and B & C).

4.2. Measuring animal paralysis rates as a surrogate for polyglutamine toxicity in muscle cells

NOTE: The age-dependent increase of polyQ aggregates in muscle causes the decline of muscular function that drives locomotion. This defect in locomotion can be determined by measuring the progressive rate of paralysis in polyQ-expressing animals. For the paralysis assay, synchronized *unc-54p::polyQ::YFP* expressing animals are scored at Day 3, 5, 7 and 9 of adulthood. Add additional time points, as needed to extend the scoring range, such that you can assess the effect of genetic perturbation.

4.2.1. On scoring days (Day 3, 5, 7 and 9 of adulthood), look at the 6 cm plates containing 50 animals and record the number of paralyzed animals. Remove paralyzed animals from the plate. If animals have crawled off the plate, or have died, they should be censored; record the event so it can be accounted for in the analysis.

NOTE: An animal is considered to be paralyzed when no movement is observed after exposing them to light or gentle touch stimuli. Pharyngeal pumping activity is used to determine whether nonmoving animals are alive or dead.

4.2.2. At the completion of the experiment, calculate the paralysis rate for each condition. Do this at each time point by dividing the fraction of paralyzed animals by the total number of animals observed for that condition at that time. If observing multiple plates per condition per time point (i.e., replicate plates), calculate the ratio separately for each replicate.

4.2.3. Plot the progression of paralysis rate in an XY plotted graph. X represents days of adulthood and Y represents paralysis rates. The paralysis rate of *unc-54p::polyQ::YFP* animals is compared to control animals (**Figure 1C**). Perform statistical analysis between the groups; for multiple trials, treat trials independently. Use the Cox Proportional-Hazards Regression and the Wald test. Most data analysis tools that support survival analysis also support Cox modeling.

4.2.4. Transform the data: each condition should have two columns, one for time, and another for "event". At each time point observed, add a row with "0" for each paralyzed animal, and a "1" for each censored animal. The total number of rows should be equal to the number of starting animals on the plate for that condition.

4.2.5. Perform Cox Proportional-Hazards modeling, followed by the Wald test, according to instructions for your statistical software. A univariate model will be appropriate for typical experiment designs. For more than two conditions, if a test with all conditions included indicates a significant result (i.e., $p < 0.005$), pairwise tests between conditions can be performed to determine the specific significant pair(s) of conditions.

NOTE: The Cox model relies on an assumption that the test condition(s) modulate the probability of an event proportionally over time. This means, for example, that the Cox model would not be appropriate for comparing a condition under which most animals are paralyzed at day 1 to a condition under which most animals are paralyzed at day 9. Extensions of the Cox model, and other approaches for comparing proportions paralyzed at each time point, are available for cases where the proportional hazards assumption does not hold, see [7-30].

5. **Measuring the decline in proteostasis in neuronal tissue by using polyglutamine expressing animals.**

NOTE: Two complementary methods are used to assay proteostasis decline in neurons (1) by quantifying the formation of protein aggregates (fluorescent foci) during aging and (2) by measuring age-associated decline in the neuronal proteome via a movement-based assay.

5.1. Imaging polyglutamine aggregate formation in the neurons during aging

NOTE: Similar to the assay already discussed in muscle tissue, the age-dependent progression of protein aggregation in the neurons is imaged by expressing a *polyQ::YFP* fusion protein driven by the pan-neuronal tissue-specific promoter of *rgef-1*. Specifically we use AM101: *rmIs110 [rgef-1p::Q40::YFP]*, a forty glutamine fusion to YFP[16]. To visualize *rgef-1p::polyQ::YFP,* use a compound microscope equipped for fluorescence with a 40x magnification lens. AM101 is available from the CGC at: https://cgc.umn.edu/strain/AM101.

5.1.1. On imaging days (Day 4, 6, 8 and 10 of adulthood), pick 20 animals and mount on a microscope slide containing a 3% agarose pad with a 5 µL drop of 10 mM sodium azide (diluted in M9 buffer).

5.1.2. After all worms are immobilized by sodium azide (~ 5 minutes), take z-stack images of the head of the animals using a 40x magnification lens (**Figure 2A**). Discard slides after imaging.

5.1.3. After acquisition of images, compress z-stacks and use to quantify the number of foci in neurons located on the nerve ring area. Foci are brighter punctuated signals that can be differentiated from the dimmer soluble signal in the background.

NOTE**:** We specifically selected the nerve ring area to quantify *rgef-1p::polyQ::YFP* aggregates since this is the region where most neurons converge to make synaptic connections. However, in order to measure levels of aggregate formation in motor neurons, *rgef-1p::polyQ::YFP* aggregates located on the dorsal or ventral nerve cord can be quantified.

5.1.4. Plot the progression of YFP foci accumulation from D4, D6, D8 and D10. Do this on an XY graph where X represents days of adulthood and Y represents number of *rgef-1p::polyQ::YFP* foci (Figure 2B). The number of foci in the experimental condition (e.g., gene downregulation or overexpression) is compared to control animals. Statistical analysis of foci counts for neurons is done in the same manner as for muscle polyQ foci; see steps 4.1.3 and the associated notes.

5.2. Measuring body bends as a surrogate measure of polyglutamine proteotoxicity in neurons.

NOTE: The proteotoxic stress induced from the progressive aggregate accumulation of neuronal polyQ is determined by looking at motor neuron defects through a thrashing assay. Quantify the number of body bends in a period of 30 seconds while suspended in M9 physiological buffer (**Supplemental File 1**).

5.2.1. On Day 2 of adulthood, pick 10 synchronized animals from the plate and place on a 10 µL drop of M9 buffer on a microscope slide. Repeat this step at least four times to get a sample of 40 or more animals.

5.2.2. Video record the movement of the 10 animals placed on the microscope slide with 10 µL of M9 buffer for a period of 30 s on a stereomicroscope with a video-capable camera. Repeat this step 4 times for a total sample number of 40. Zoom and position should be adjusted such that all the animals are visible in the frame for the full 30 seconds.

5.2.3. Once all the videos with the animals to be analyzed are recorded, play the video and score the body bends of each animal. One body bend is defined as when the vulva of the animal goes from one side to the opposite and all the way back to the starting position.

NOTE: We find wild type animals typically have 49 ± 0.79 body bends in 30 seconds.

5.2.4. Plot the number of body bends for each animal in a column graph where each dot represents the number of body bends in 30 s (Y axis) with the different conditions tested on the X axis. The number of body bends of *unc-54p::polyQ::YFP* animals is compared to control animals (**Figure 2C**). Perform statistical analysis between the groups independently for each trial; if the assay is repeated at multiple time points, analyze the data independently for each time point.

5.2.4.1. When considering only two conditions, perform an independent-sample t-test.

5.2.4.2. When considering more than two conditions at once, first perform an omnibus one-way ANOVA analysis, including the data for all the conditions at that time trial/time point. If the omnibus ANOVA yields a significant p-value (i.e., $p < 0.005$), perform a *post-hoc* analysis with pairwise independent sample t-tests to determine the specific conditions between which a significant difference in body bend count was detected.

REPRESENTITIVE RESULTS:

In *C. elegans*, the polyglutamine repeat model has been instrumental for the identification of genes that regulate the proteostatic network. For instance, we previously showed that the homeodomain interacting protein kinase (*hpk-1*), a transcriptional cofactor, influences proteostasis during aging by regulating expression of autophagy and molecular chaperones[31]. We found that loss of *hpk-1*, either by RNAi silencing or in *hpk-1(pk1393)* null mutant animals, increases the number of *Q35::YFP* aggregates that accumulate during aging. Day 2 adult control animals display 18.0 ± 2.7 aggregates while the *hpk-1(pk1393)* null mutant and *hpk-1* RNAi-treated *Q35::YFP* animals averaged 28 ± 5.3 and 26.0 ± 5.1 aggregates, respectively (**Figure 3A-D**). Similarly, by day 8 of adulthood, 77–78% of *hpk-1(RNAi)* and *hpk-1(pk1393)* animals were paralyzed while 50% of control *Q35*::*YFP* animals were paralyzed (**Figure 3E**). In addition, HPK-1 is sufficient to regulate protein aggregate formation as ubiquitous overexpression of *hpk-1* reduces the number of *Q35::YFP* in muscle tissue and protects aging animals from *Q35*::*YFP*-associated paralysis during aging (**Figure 3E**). Collectively, these results demonstrate that HPK-1 regulates proteostasis and highlights how the polyQ::YFP model can be utilized for reverse genetic analysis of changes in proteostasis during aging.

FIGURE AND TABLE LEGENDS:

Figure 1. Expression of *polyQ::YFP* within *C. elegans* muscle results in progressive foci accumulation and paralysis during aging. (**A**) *C. elegans unc-54p::Q35::YFP* expression at days 1 and 4 of adulthood (upper and lower panel, respectively). Arrows indicate representative foci. (**B**) Quantification of fluorescent foci over the first 4 days of adulthood. Foci are resistant to FRAP [15,32,33], consistent with an insoluble protein aggregate. Error bars represent standard error of the mean (SEM) (**C**) *unc-54p::Q35::YFP* animals become paralyzed during aging. Error bars represent standard error of proportion. Raw data for (**B-C**) is provided in **Supplemental Table 1**. The scale bar represents 100 µm in all panels.

Figure 2. Expression of *polyQ::YFP* within *C. elegans* neurons results in progressive foci accumulation and disruption of normal body bends. (**A, top**) DIC image of the *C. elegans* anterior. The pharynx is a bi-lobed structure in the head of the animal, which is surrounded by the nerve ring, an interconnected cluster of 180 neurons. Red brackets indicate region to score for foci within head neurons. (**A, middle**) *rgefp-1::Q40::YFP* fluorescence at day 2 adulthood. Note that YFP expression is largely diffuse, with the exception of an occasional aggregate (arrow). (**A, bottom**) *rgefp-1::Q40::YFP* fluorescence at day 10 adulthood. Foci/aggregates are indicated (red arrow). (**B**) Quantification of fluorescent foci over the first 10 days of adulthood. Foci are resistant to FRAP [15,32,33], consistent with an insoluble protein aggregate. Error bars represent standard error of the mean (**C**) Typical frequency of body bends of *wild type* and *rgef-1p::Q40::YFP* animals maintained at 20°C feeding on empty vector RNAi (L4440) at days 2 adulthood. Increased glutamine expansion correlates with movement defects[15]. Error bars represent standard error of the mean. Raw data for (**B-C**) is provided in **Supplemental Table 1**. The scale bar represents 20 μm in all panels.

Figure 3. HPK-1 promotes proteostasis. (**A-C**) *hpk-1* activity affects the accumulation of Q35::YFP foci in muscle cells. Shown are representative images of *Punc-54::polyQ::YFP* animals treated with (**A**) control RNAi or (**B**) *hpk-1* RNAi*,* and (**C**) transgenic animals overexpressing *hpk-1* (*Psur-5::HPK-1::CFP*). (**D**) Time course of polyQ::YFP foci accumulation in conjunction with: treatment with control RNAi (black circles), *hpk-1* RNAi (white circles), *hpk-1(pk1393)* (white squares), or *hpk-1* overexpression (open triangles). Data points display the mean ± standard deviation (S.D.) of at least 15 animals per biological replicate; at least 5 independent experiments were performed. (**E**) Time course of paralysis of *Punc-54::polyQ::YFP* animals in conjunction with: treatment with control RNAi (black circles), *hpk-1* RNAi (white circles), *hpk-1(pk1393)* (white squares), or *hpk-1* overexpression (open triangles). Plotted data display the results for a single representative trial. This figure is reprinted from reference[31] with permission via a Creative Commons Attribution (CC BY) license. The scale bar represents 100 μm in all panels.

Supplemental Table 1. Raw data of results. Table includes foci, paralysis, and body bend data from Figures 2 and 3.

Supplemental File 1. Common reagents for routine *C. elegans* work. Common reagents include recipes for preparing various types of plates and buffers.

DISCUSSION:

Aging is characterized by a gradual decline in proteostasis. Proteostasis is maintained by a complex system, the proteostatic network, for the coordinated, dynamic, stress-responsive control of protein folding, degradation, and translation. Why proteostasis fails in the course of aging is poorly understood, but a decaying epigenome, declining inducibility of stress responses, and loss of compensatory crosstalk all coincide with this breakdown. In *C. elegans,* the transcriptional inducibility of multiple forms of stress response rapidly decline within a few hours after the onset of reproduction due to the formation of repressive chromatin marks at stress loci[2,34,35]. Proteostasis collapse is a massive clinical problem as it underlies the development of protein misfolding diseases. Thus, having a method suitable to genetic analysis to quantify

cellular proteostasis in vivo is essential to gain deeper mechanistic insight into how organisms maintain proper folding and function of the proteome.

Transgenic *C. elegans* with tissue-specific expression of a polyglutamine fluorescent reporter are an effective and robust method to study age-dependent decline of proteostasis. The two most prominent benefits of the polyglutamine model are: (1) tissue-specific expression combined with powerful genetics and functional genomics allows discovery and characterization of proteostasis regulators in the context of an intact multicellular organism, and (2) visualization of foci formation permits direct quantification of age-associated proteostatic decline in vivo. While in many cases a correlation exists between aggregate accumulation and increased proteotoxicity, in some instances, these two phenotypes are negatively correlated. For example, decreased insulin signaling increases lifespan and stress resistance: *daf-2* mutant animals (a hypomorphic loss of function in the insulin/insulin-like growth factor 1 receptor), show an increased aggregate load while improving proteostasis capacity by the upregulation of a protective mechanism that prevents the formation of toxic aggregate species[33,36-39]. Thus, in some cases aggregate formation is protective by sequestering harmful protein species from the rest of the proteome. Since readouts of cellular proteotoxicity can be assessed in conjunction with aggregate formation, one can test for inverse correlations to identify genetic interactions involved in protective sequestration mechanisms. Lastly, polyglutamine fluorescent reporters can be combined with either tissue specific knockdown (e.g., classically through tissue specific RNAi or RNA hairpin expression), and more recently through tissue-specific protein degradation, such as the Tir1-auxin system[40]- or with tissue-specific overexpression of a gene of interest using tissue-specific reporters, thereby gaining insight into regulation of proteostasis within and across cells and tissues.

Methods to measure changes in proteostasis during aging require chronologically matched animals. Thus, it is necessary to either prevent production of offspring or to separate starting animals. In the protocol, we outline how to use FUdR to prevent progeny production, but some studies have reported that FUdR can alter proteostasis[24,25]. Alternatively, feminized genetic backgrounds can be used (e.g., *fer-15(b26);fem-1(hc17)*[41]). Lastly, adult animals can be moved to fresh RNAi plates away from progeny. This simplifies background considerations at the expense of throughput. Periodically moving animals to fresh food has the additional advantages of renewing exposure to dsRNA and preventing possible starvation.

Because fluorescent foci are quantified through visual observation, one must be precise and consistent in the identification of foci. *C. elegans polyQ::YFP* foci have been experimentally verified to be in vivo protein aggregates via fluorescence recovery after photobleaching (FRAP)[15,32,33]. Additional biochemical approaches can be used to assess protein aggregation[42]. It is important to note that by day 3 adulthood, early foci become larger and begin to accumulate what appear as satellite foci (analogous to moons around a planet). It is essential to decide before beginning whether to count these satellite foci as separate aggregates, or to be more conservative and consider the collective area as a single aggregate, and then to remain consistent when scoring throughout all experiments. We prefer the latter; it extends the dynamic range during which foci formation can be assessed, but even with these more conservative estimates,

by day 4 – 5 there is an apparent plateau effect. In actuality proteostasis continues to decline, but foci are so numerous it is no longer possible to quantify the number accurately by eye. To improve reproducibility across biological trials, between individuals, and between laboratories, it is critical to define what is being scored as foci.

While we detail methods for simple reverse genetic approaches to test a limited set of conditions for changes in proteostasis using the *unc-54p::Q35::YFP* reporter, we have developed methods with higher throughput where changes in proteostasis can be quantified for up to 100 conditions (e.g., RNAi clones) simultaneously. This method involves the use of replica sets, which we have used extensively to quantify changes in lifespan after genetic perturbation. Briefly, independent samples derived from a large isogenic population are scored at each timepoint, rather than a single sample over time. This approach is easily adapted for assessing age-associated proteotoxic changes, such as paralysis (using the poly-Q::YFP with the muscle promoter) or body bends (via neuronal promoter). Replica set scoring in this manner entails adding liquid to the wells of a multi-well plate, which stimulates *C. elegans* to move. An analogous approach can be readily applied to foci formation within muscle cells. Previously, we identified 159 genes necessary for a normal (wild-type) lifespan or the increased lifespan of decreased insulin/IGF1 receptor mutant animals, and quantified changes in healthspan and lifespan. Of these, 103 gene inactivations result in a progeric phenotype, with animals showing one or more signs of premature aging[43]. In a secondary screen using the *unc-54p::Q35::YFP* reporter and a replica set scoring approach, we were able to identify approximately 50 progeric gene inactivations that produced accelerated foci formation (A.V.S. unpublished results), which subsequently facilitated focused mechanistic studies where we identified a critical role for both the Myc network of transcription factors and the transcriptional co-factor HPK-1 in maintaining proteostasis[31,44]. A detailed description of the replica set method can be found in[23].

The methods described here for statistical analysis of polyQ foci across conditions focus on comparing conditions within each time point, however there may be cases where the trend across time is of more interest than a comparison at a single point. If it is possible to track individual animals over time, such as if animals are singled in wells of multi-well plates or microfluidic devices, a relatively simple repeated-measures ANOVA would be appropriate. However, most often animals are kept in bulk on petri plates, making such individual tracking infeasible, and thus different methods are needed. The polyQ aggregate count data is expected to be autocorrelated between time points (e.g., foci counts should only increase, making observations for a given condition not independent between time points), necessitating a statistical analysis approach which can appropriately handle correlated error, such as ARIMA.

Both foci formation and movement defects are well-defined and quantifiable molecular hallmarks of aging that are tractable to genetic and/or functional genomic analysis. For example, a forward genetic screen using *C. elegans* expressing *Q35::YFP* within muscle cells identified enhanced aggregation after loss of *unc-30*, a neuron-specific transcription factor that regulates the synthesis of the inhibitory neurotransmitter gamma-aminobutyric acid (GABA)[32]. The development of feeding-based RNAi in *C. elegans* also led to a period of gene discovery in proteostasis: a genome-wide RNAi screens of *C. elegans* expressing *Q35::YFP* identified

approximately 340 genetic modifiers that either enhance or inhibit the proteostatic network and thus increase or decrease polyQ aggregation[39,42].

While straightforward functional genomic screens revealed a core proteostatic network, these strains remain an invaluable phenotypic resource. Tissue-specific expression of polyglutamine fluorescent reporters in *Caenorhabditis elegans* is an ideal system in which established genetic and functional genomic tools can be applied via enhancer, suppressor, or synthetic screens to identify novel genetic interactions[45,46]. Cellular proteostasis, and the myriad physiological systems that operate either to preserve or to challenge overall protein homeostasis, is emerging as a complicated cell biological and endocrine picture. Proteostasis is not represented by a single biological pathway, protein complex, or organelle. Instead, proteostasis is the product of the mass action of multiple intricate and interdependent biological pathways, machines and systems, and is challenged by myriad environmental stressors. Future studies utilizing the *polyQ::YFP* model will be essential to unravel the complexity of how cells maintain proper function and folding of the proteome.

ACKNOWLEDGEMENTS:

We would like to thank past and present members of the Samuelson laboratory for their assistance in the refinement of this method and/or discussion that aided the development of this manuscript. Research reported in this publication was supported by the National Institute on Aging of the National Institutes of Health under Award Numbers RF1AG062593 and R21AG064519. The content is solely the responsibility of the authors and does not necessarily represent the official views of the National Institutes of Health. The funders had no role in study design, data collection and analysis, decision to publish, or preparation of the manuscript.

DISCLOSURES:

The authors declare that they have no competing financial interests.

REFERENCES:

1 Wolff, S., Weissman, J. S., Dillin, A. Differential scales of protein quality control. *Cell.* **157** (1), 52-64 (2014).

2 Labbadia, J., Morimoto, R. I. The biology of proteostasis in aging and disease. *Annual Review of Biochemistry.* **84** 435-464 (2015).

3 Powers, E. T., Morimoto, R. I., Dillin, A., Kelly, J. W., Balch, W. E. Biological and chemical approaches to diseases of proteostasis deficiency. *Annual Review of Biochemistry.* **78** 959-991 (2009).

4 Brehme, M. et al. A chaperome subnetwork safeguards proteostasis in aging and neurodegenerative disease. *Cell Reports.* **9** (3), 1135-1150 (2014).

5 Sala, A. J., Bott, L. C., Morimoto, R. I. Shaping proteostasis at the cellular, tissue, and organismal level. *Journal of Cell Biology.* **216** (5), 1231-1241 (2017).

6 Braak, H., Braak, E., Strothjohann, M. Abnormally phosphorylated tau protein related to the formation of neurofibrillary tangles and neuropil threads in the cerebral cortex of sheep and goat. *Neuroscience Letters.* **171** (1-2), 1-4 (1994).

7 Poirier, M. A., Jiang, H., Ross, C. A. A structure-based analysis of huntingtin mutant polyglutamine aggregation and toxicity: evidence for a compact beta-sheet structure. *Human Molecular Genetics.* **14** (6), 765-774 (2005).
8 Vilchez, D., Saez, I., Dillin, A. The role of protein clearance mechanisms in organismal ageing and age-related diseases. *Nature Communications.* **5** 5659 (2014).
9 Eftekharzadeh, B., Hyman, B. T., Wegmann, S. Structural studies on the mechanism of protein aggregation in age related neurodegenerative diseases. *Mechanisms of Ageing and Development.* **156** 1-13 (2016).
10 Pokrishevsky, E., Grad, L. I., Cashman, N. R. TDP-43 or FUS-induced misfolded human wild-type SOD1 can propagate intercellularly in a prion-like fashion. *Scientific Reports.* **6** 22155 (2016).
11 Mukherjee, A., Morales-Scheihing, D., Butler, P. C., Soto, C. Type 2 diabetes as a protein misfolding disease. *Trends in Molecular Medicine.* **21** (7), 439-449 (2015).
12 Sikkink, L. A., Ramirez-Alvarado, M. Biochemical and aggregation analysis of Bence Jones proteins from different light chain diseases. *Amyloid.* **15** (1), 29-39 (2008).
13 Qu, B. H., Strickland, E., Thomas, P. J. Cystic fibrosis: a disease of altered protein folding. *Journal of Bioenergetics and Biomembranes.* **29** (5), 483-490 (1997).
14 Qu, B. H., Strickland, E. H., Thomas, P. J. Localization and suppression of a kinetic defect in cystic fibrosis transmembrane conductance regulator folding. *Journal of Biological Chemistry.* **272** (25), 15739-15744 (1997).
15 Brignull, H. R., Moore, F. E., Tang, S. J., Morimoto, R. I. Polyglutamine proteins at the pathogenic threshold display neuron-specific aggregation in a pan-neuronal Caenorhabditis elegans model. *Journal of Neuroscience.* **26** (29), 7597-7606 (2006).
16 Gidalevitz, T., Ben-Zvi, A., Ho, K. H., Brignull, H. R., Morimoto, R. I. Progressive disruption of cellular protein folding in models of polyglutamine diseases. *Science.* **311** (5766), 1471-1474 (2006).
17 Morimoto, R. I. Stress, aging, and neurodegenerative disease. *New England Journal of Medicine.* **355** (21), 2254-2255 (2006).
18 Morimoto, R. I. Proteotoxic stress and inducible chaperone networks in neurodegenerative disease and aging. *Genes & Development.* **22** (11), 1427-1438 (2008).
19 Walker, F. O. Huntington's disease. *Lancet.* **369** (9557), 218-228 (2007).
20 Kamath, R. S., Martinez-Campos, M., Zipperlen, P., Fraser, A. G., Ahringer, J. Effectiveness of specific RNA-mediated interference through ingested double-stranded RNA in Caenorhabditis elegans. *Genome Biology.* **2** (1), RESEARCH0002. (2001).
21 Karady, I. et al. Using Caenorhabditis elegans as a model system to study protein homeostasis in a multicellular organism. *Journal of Visualized Experiments.* 10.3791/50840 (82), e50840 (2013).
22 Porta-de-la-Riva, M., Fontrodona, L., Villanueva, A., Ceron, J. Basic Caenorhabditis elegans methods: synchronization and observation. *Journal of Visualized Experiments.* 10.3791/4019 (64), e4019 (2012).
23 Cornwell, A. B., Llop, J. R., Salzman, P., Thakar, J., Samuelson, A. V. The Replica Set Method: A High-throughput Approach to Quantitatively Measure Caenorhabditis elegans Lifespan. *Journal of Visualized Experiments.* 10.3791/57819 (136) (2018).

24 Angeli, S. et al. A DNA synthesis inhibitor is protective against proteotoxic stressors via modulation of fertility pathways in Caenorhabditis elegans. *Aging (Albany NY).* **5** (10), 759-769 (2013).
25 Feldman, N., Kosolapov, L., Ben-Zvi, A. Fluorodeoxyuridine improves Caenorhabditis elegans proteostasis independent of reproduction onset. *PLoS One.* **9** (1), e85964 (2014).
26 Byerly, L., Cassada, R. C., Russell, R. L. The life cycle of the nematode Caenorhabditis elegans. I. Wild-type growth and reproduction. *Developmental Biology.* **51** (1), 23-33 (1976).
27 Schemper, M. Cox Analysis of Survival Data with Non-Proportional Hazard Functions. *Journal of the Royal Statistical Society. Series D (The Statistician).* **41** (4), 455-465 (1992).
28 Royston, P., Parmar, M. K. The use of restricted mean survival time to estimate the treatment effect in randomized clinical trials when the proportional hazards assumption is in doubt. *Statistics in Medicine.* **30** (19), 2409-2421 (2011).
29 Campbell, I. Chi-squared and Fisher-Irwin tests of two-by-two tables with small sample recommendations. *Statistics in Medicine.* **26** (19), 3661-3675 (2007).
30 Busing, F. M., Weaver, B., Dubois, S. 2 x 2 Tables: a note on Campbell's recommendation. *Statistics in Medicine.* **35** (8), 1354-1358 (2016).
31 Das, R. et al. The homeodomain-interacting protein kinase HPK-1 preserves protein homeostasis and longevity through master regulatory control of the HSF-1 chaperone network and TORC1-restricted autophagy in Caenorhabditis elegans. *PLoS Genetics.* **13** (10), e1007038 (2017).
32 Garcia, S. M., Casanueva, M. O., Silva, M. C., Amaral, M. D., Morimoto, R. I. Neuronal signaling modulates protein homeostasis in Caenorhabditis elegans post-synaptic muscle cells. *Genes & Development.* **21** (22), 3006-3016 (2007).
33 Morley, J. F., Brignull, H. R., Weyers, J. J., Morimoto, R. I. The threshold for polyglutamine-expansion protein aggregation and cellular toxicity is dynamic and influenced by aging in Caenorhabditis elegans. *Proceedings of the National Academy of Sciences of the United States of America.* **99** (16), 10417-10422. (2002).
34 Labbadia, J., Morimoto, R. I. Repression of the Heat Shock Response Is a Programmed Event at the Onset of Reproduction. *Molecular Cell.* **59** (4), 639-650 (2015).
35 Shemesh, N., Shai, N., Ben-Zvi, A. Germline stem cell arrest inhibits the collapse of somatic proteostasis early in Caenorhabditis elegans adulthood. *Aging Cell.* **12** (5), 814-822 (2013).
36 Ben-Zvi, A., Miller, E. A., Morimoto, R. I. Collapse of proteostasis represents an early molecular event in Caenorhabditis elegans aging. *Proceedings of the National Academy of Sciences of the United States of America.* **106** (35), 14914-14919 (2009).
37 Walther, D. M. et al. Widespread Proteome Remodeling and Aggregation in Aging C. elegans. *Cell.* **161** (4), 919-932 (2015).
38 Cohen, E., Bieschke, J., Perciavalle, R. M., Kelly, J. W., Dillin, A. Opposing activities protect against age-onset proteotoxicity. *Science.* **313** (5793), 1604-1610 (2006).
39 Silva, M. C. et al. A genetic screening strategy identifies novel regulators of the proteostasis network. *PLoS Genetics.* **7** (12), e1002438 (2011).
40 Zhang, L., Ward, J. D., Cheng, Z., Dernburg, A. F. The auxin-inducible degradation (AID) system enables versatile conditional protein depletion in C. elegans. *Development.* **142** (24), 4374-4384 (2015).

41 Hansen, M., Hsu, A. L., Dillin, A., Kenyon, C. New genes tied to endocrine, metabolic, and dietary regulation of lifespan from a Caenorhabditis elegans genomic RNAi screen. *PLoS Genetics.* **1** (1), 119-128 (2005).
42 Nollen, E. A. et al. Genome-wide RNA interference screen identifies previously undescribed regulators of polyglutamine aggregation. *Proceedings of the National Academy of Sciences of the United States of America.* **101** (17), 6403-6408 (2004).
43 Samuelson, A. V., Carr, C. E., Ruvkun, G. Gene activities that mediate increased life span of C. elegans insulin-like signaling mutants. *Genes & Development.* **21** (22), 2976-2994 (2007).
44 Johnson, D. W. et al. The Caenorhabditis elegans Myc-Mondo/Mad complexes integrate diverse longevity signals. *PLoS Genetics.* **10** (4), e1004278 (2014).
45 Wang, Z., Sherwood, D. R. Dissection of genetic pathways in C. elegans. *Methods in Cell Biology.* **106** 113-157 (2011).
46 Jorgensen, E. M., Mango, S. E. The art and design of genetic screens: caenorhabditis elegans. *Nature Reviews Genetics.* **3** (5), 356-369 (2002).

Figure 1

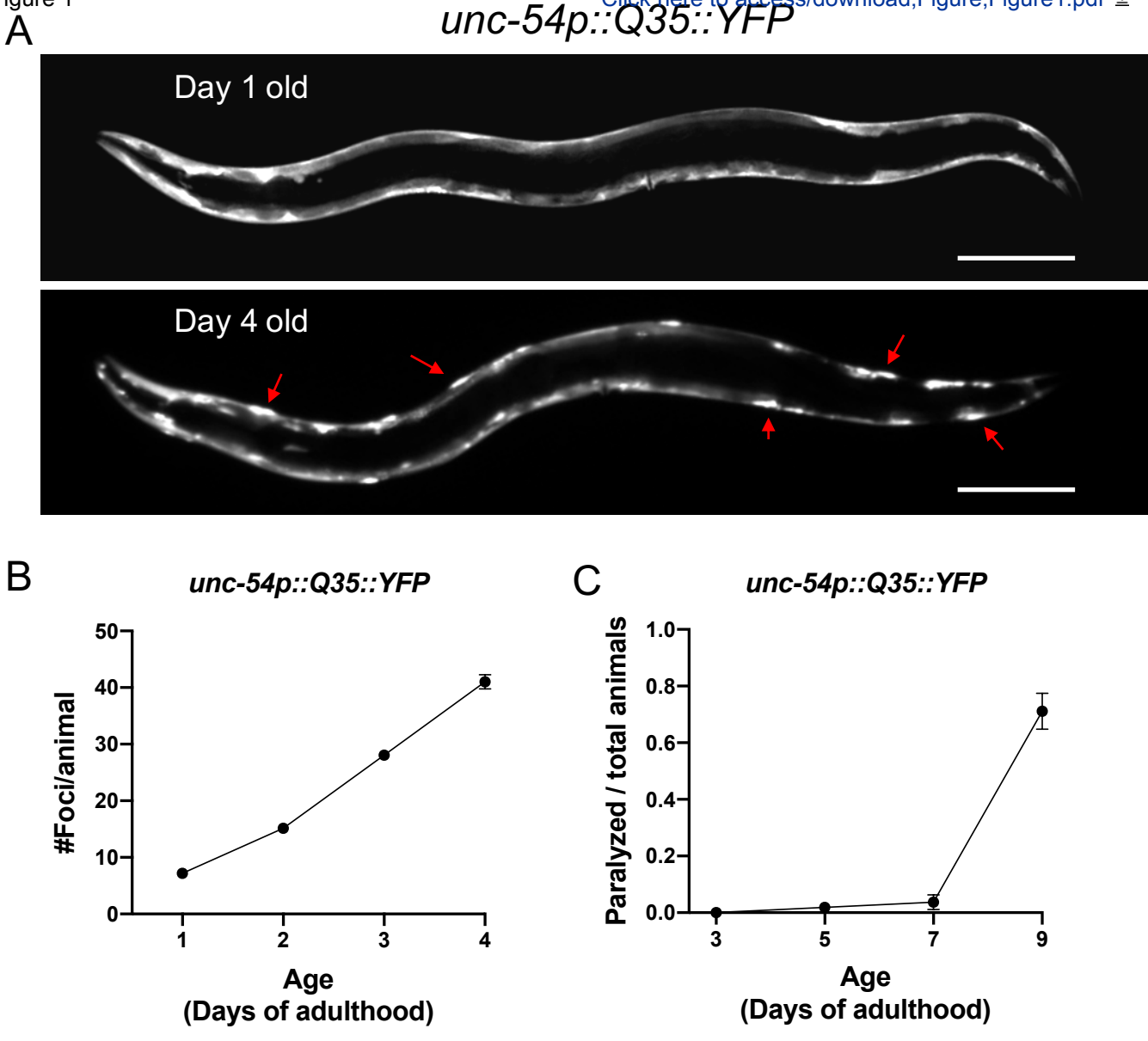

Figure 2

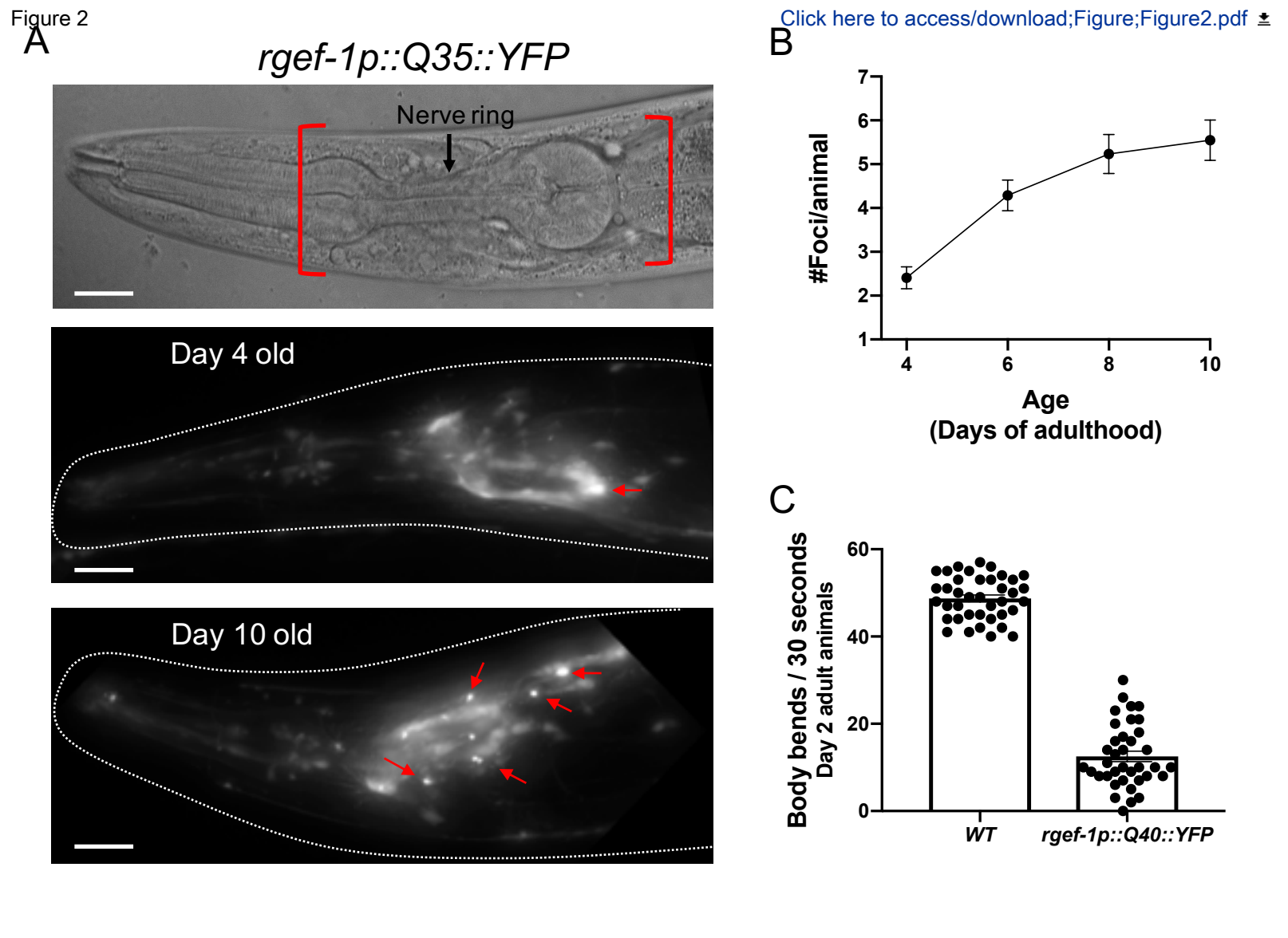

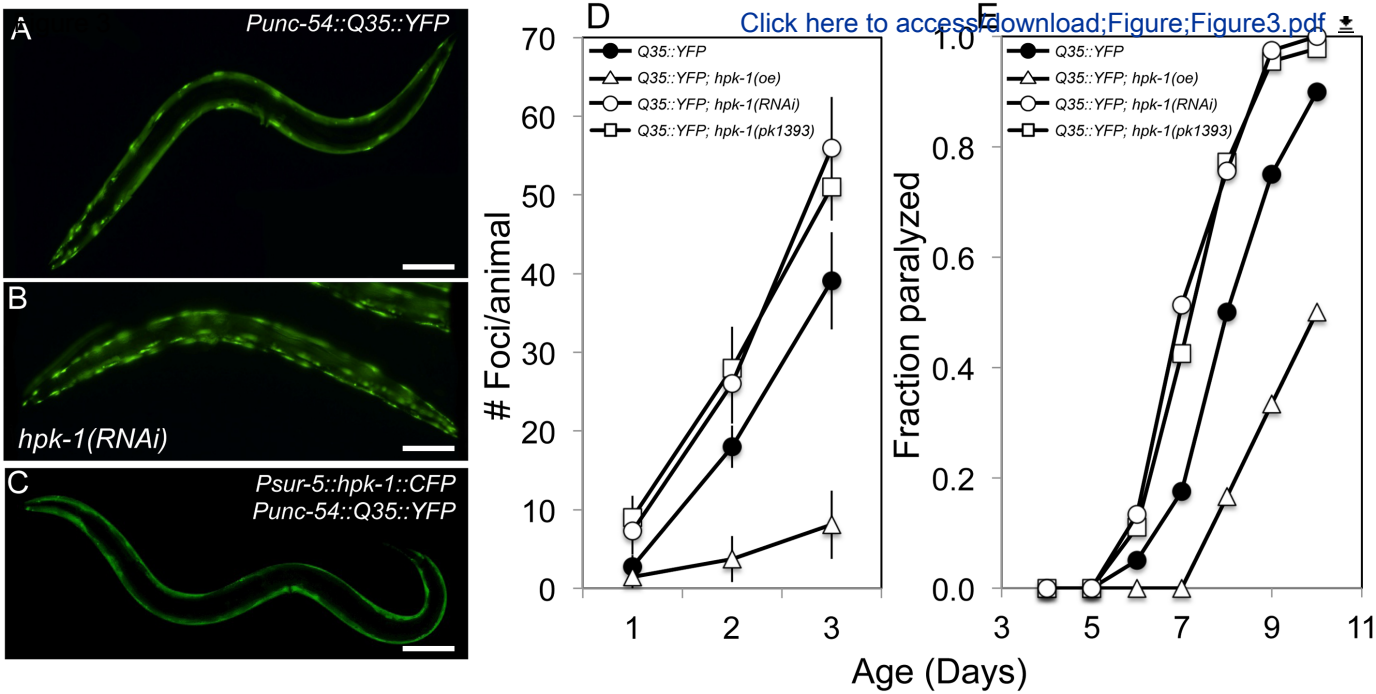

Name of Material/ Equipment	Company	Catalog Number
24 Well Culture Plates	Greiner Bio-One	#662102
2 mL 96-well plates	Greiner Bio-One	#780286
600 µL 96-well plates	Greiner Bio-One	#786261
96-pin plate replicator	Nunc	250520
Air-permeable plate seal	VWR	60941-086
bacteriological agar	Affymetrix/USB	10906
bacto-peptone	VWR	90000-368
C. elegans RNAi clone library in HT115 bacteria- Ahringer	Source Bioscience	C. elegans RNAi Collection (Ahringer)
C. elegans RNAi clone library in HT115 bacteria- Vidal	Source Bioscience	C. elegans ORF-RNAi Resource (Vidal)
FuDR (5-Fluoro-2'-deoxyuridine)	Alfa Aesar	L16497
Glass microscope cover slips	VWR	48404-455
Glass microscope slides	VWR	160004-422
IPTG (isopropyl beta-D-1-thigalactopyranoside)	Gold Bio	12481C100
Retangular non-treated single-well plate, 128x86mm	Thermo-Fisher	242811
Sodium Azide, CAS #26628-22-8	Sigma-Aldrich	S2002
Zeiss Axio Imager M2m microscope with AxioVision v4.8.2.0 software	Zeiss	unknown
Zeiss StemiSV11 M2 Bio Quad microscope	Zeiss	unknown

Comments/Description

See also Kamath et. al, Nature 2003.

See also Rual et. al, Genome Research 2004. This library is also available from Dharmacon.

Detailed comments to the critique
Response to Editorial Comments.

1. Please take this opportunity to thoroughly proofread the manuscript to ensure that there are no spelling or grammatical errors.

We have proofread the manuscript.

2. Please ensure that all text in the protocol section is written in the imperative voice/tense as if you are telling someone how to do the technique (i.e. "Do this", "Measure that" etc.) Any text that cannot be written in the imperative tense may be added as a "Note", however, notes should be used sparingly and actions should be described in the imperative tense wherever possible.

We have made the required changes.

1) Lines 151-155 need to be rewritten in the imperative voice and made into steps.

We have rewritten these lines.

2) 2.1: Unclear if this is a title or step.

It is a step. The redaction of this step was corrected to make it clear.

3. Please note that your protocol will be used to generate the script for the video, and must contain everything that you would like shown in the video. ***Please add more specific details (e.g. button clicks for software actions, numerical values for settings, etc) to your protocol steps.*** *There should be enough detail in each step to supplement the actions seen in the video so that viewers can easily replicate the protocol. Some examples:*
1) 1.1: unclear how the genes are identified, and what we can film here. Please clarify.
2) 1.3.1: Use g for all centrifuge speeds

1.1 The text was changed from "identify" to "select" the genes that are going to be used by the researcher to inactivate expression by RNAi. The genes to be selected depends on the researcher interest.
1.3.1 The rotational speed has been changed to RCF (g).

4. Please add a one-line space after each protocol step.

We have made the required changes.

5. After you have made all of the recommended changes to your protocol (listed above), please re-evaluate the length of your protocol section. There is a 10-page limit for the protocol text, and a 3- page limit for filmable content. If your protocol is longer than 3 pages, please highlight ~2.5 pages or less of text (which includes headings and spaces) in yellow, to identify which steps should be visualized to tell the most cohesive story of your protocol steps.

601 Elmwood Avenue • Box 633 • Rochester, NY 14642
585-273-2409 • 585-273-1450 fax • andrew_samuelson@urmc.rochester.edu

In the revised manuscript, the protocol section is 7 pages long and the filmable content is 3 pages long.

1) The highlighting must include all relevant details that are required to perform the step. For example, if step 2.5 is highlighted for filming and the details of how to perform the step are given in steps 2.5.1 and 2.5.2, then the sub-steps where the details are provided must be included in the highlighting.

We checked the article to make sure that all steps have the appropriate sub-steps highlighted.

2) The highlighted steps should form a cohesive narrative, that is, there must be a logical flow from one highlighted step to the next.

We have made the required changes.

3) Please highlight complete sentences (not parts of sentences). Include sub-headings and spaces when calculating the final highlighted length.

We have made the required changes.

4) Notes cannot be filmed and should be excluded from highlighting.

We have made the required changes.

6. JoVE articles are focused on the methods and the protocol, thus the discussion should be similarly focused. Please ensure that the discussion covers the following in detail and in paragraph form (3-6 paragraphs): 1) modifications and troubleshooting, 2) limitations of the technique, 3) significance with respect to existing methods, 4) future applications and 5) critical steps within the protocol.

Thank you pointing this out. We have highlighted (as a comment) how each paragraph of the discussion addresses the aforementioned criteria. We apologize for the length of our discussion, but as Reviewer 1 has noted (point 1 below): this protocol is commonly used by *C. elegans* proteostasis aficionados and we felt that it was important to emphasize the continued relevance of this method and highlight future modification and application of this method. While some details could be moved to the main text (e.g. alternatives to the use of FUDR), we were guided in their placement based on out previous JoVE publication (*Cornwell et al. 2018*) and comments from the reviewers.

7. *Please spell out journal names.*

We apologize for the error. We have applied the JoVE-1 style in Endnote X8:
(https://www.jove.com/files/JoVE.ens).

8. If your figures and tables are original and not published previously or you have already obtained

601 Elmwood Avenue • Box 633 • Rochester, NY 14642
585-273-2409 • 585-273-1450 fax • andrew_samuelson@urmc.rochester.edu

figure permissions, please ignore this comment. If you are re-using figures from a previous publication, you must obtain explicit permission to re-use the figure from the previous publisher (this can be in the form of a letter from an editor or a link to the editorial policies that allows you to re-publish the figure). Please upload the text of the re-print permission (may be copied and pasted from an email/website) as a Word document to the Editorial Manager site in the "Supplemental files (as requested by JoVE)" section. Please also cite the figure appropriately in the figure legend, i.e. "This figure has been modified from [citation]."

Figures 1 & 2 are original, generated for this manuscript.
Figure 3 was published in PLoS Genetics in 2017. PLoS states (https://www.plos.org/license):

> "PLOS applies the Creative Commons Attribution (CC BY) license to works we publish. Under this license, authors retain ownership of the copyright for their content, but they allow anyone to download, reuse, reprint, modify, distribute and/or copy the content as long as the original authors and source are cited."

In the Figure legend for Figure 3 we state: "This figure is reprinted from reference [31] with permission via a Creative Commons Attribution (CC BY) license." (lines 401-402).

Response to Reviewer #1.

1. This manuscript is somewhat unsatisfying as it does not present a major advancement of a common protocol. The counting of polyQ foci is performed in numerous publications as a very basic tool to access general proteostasis and may not justify an extra protocol. The authors used two published strains by the Morimoto lab and their own contribution was solely the crossing with the hpk-1 oe line (+ RNAi) that was also already published.

We thank the reviewer for raising this concern. While this protocol is commonly used by *C. elegans* investigators in the proteostasis field, we agreed to contribute this protocol to the collection to: further advocate the continued use of these strains, highlight their versatility and relevance, and to lower the barrier for their use by scientists that are new to the field. As the reviewer is aware, the Morimoto laboratory was one of the labs that founded the field of proteostasis. We enthusiastically advocate for the use and continued relevance of these tools in aging and proteostasis research! We tried to strike a neutral tone in the original submission, but should the reviewer desire, we are happy advocate further and cite more relevant references to give additional credit for the development and use of these tools.

We apologize if the reviewer is under the impression that we are claiming undue credit. We do not seek to claim credit for the advent of this method, only to advocate on its value. Our laboratory's use of these tools to contribute to the field of proteostasis is relatively modest: two publications from our laboratory in PLoS Genetics used these strains (*Johnson et al. 2014 PMID: 24699255 and Das et al. 2017 PMID: 29036198*), in which we identified and characterized novel transcriptional regulators of the proteostatic network. Nonetheless, we believe we have demonstrated sufficient expertise to contribute to this collection.

We chose to adhere to the outlines of the initial solicitation from the guest editors:

601 Elmwood Avenue • Box 633 • Rochester, NY 14642
585-273-2409 • 585-273-1450 fax • andrew_samuelson@urmc.rochester.edu

> "*We hope that this Methods Collection will be the definitive record of techniques to set the standard for reproducibility within the community. We are aiming to cover standard and advanced experimental approaches to monitor proteostasis at the molecular, cellular and organismal level in C. elegans.*"

We made the decision to limit our method to standard approaches that have gone through peer review. As we mention in the discussion, we have used a modified higher-throughput version of this method to simultaneously quantify age-associated changes in proteostasis for over 100 RNAi clones that produce premature aging phenotypes and have a manuscript in preparation of these findings. We did not add this to the primary methods section in the original submission because our results are unpublished, but believe this article will help to "pave the way" for our forthcoming study and as currently discussed provides an example of "modifications and future applications", which is in line with JoVE's expectations for a discussion.

Finally, we believe our article is worthwhile based on JoVE's FAQ page:

> "JoVE videos are a unique and effective tool to learn and share a particular technique. We are primarily concerned about publishing highly reproducible methodologies regardless of novelty. These methodologies can be previously published protocols or new techniques. Previously published protocols must be properly cited. Please note that results for experiments can be representative."

2. In addition, the presented data would be more comprehensive if the control lines: unc-54::YFP and rgef-1::YFP would have been analyzed in parallel - this should also be pointed out to the readers. Both control strains were generated by the Morimoto lab as well and are available. So the extra work is negligible.

We thank the reviewer for their comment. Our experiments were done in parallel for both reporters (*unc-54::Q35::YFP* and *rgef-1::Q40::YFP*), but the days we used for foci quantification were different because the polyQ aggregates in the nervous system form later in adulthood (after D4) compared to polyQ aggregates in the muscle (after D1).

3. Some spelling mistakes and typos can be found: e.g. line 196: instead of unc-54::G35::YFP it should read: unc-54::Q35::YFP.

We thank the reviewer and have corrected these mistakes.

Response to Reviewer #2.

1. The method include a section on Synchronization of C. elegans that involves hypochlorite treatment of gravid adults, While this method as stated as many advantages in the ease of getting synchronized population of worms, it causes stress to the animals and can impact regulators of

601 Elmwood Avenue • Box 633 • Rochester, NY 14642
585-273-2409 • 585-273-1450 fax • andrew_samuelson@urmc.rochester.edu

proteostasis (Karady et al 2013, J. Vis. Exp. (82), e50840), similar to the use of FUdR that is discussed here.

We thank the reviewer for pointing this out to us, and agree that hypochlorite treatment may impact proteostasis. However, we looked at the *Karady et al.* manuscript in depth and while it states that synchronization via hypochlorite causes stress and affects proteostasis, the manuscript does not actually demonstrate the validity of this claim nor does that manuscript provide a reference. To our surprise, after looking through other papers from the Ben-Zvi lab, and conducting a broader literature search, we could not find actual evidence demonstrating that bleaching affects proteostasis. We would welcome any additional insight to identify the specific relevant study. Nevertheless, we agree that this is a potential concern and have included a cautionary note about hypochlorite treatment in the "Synchronization of *C. elegans*" section and referenced the aforementioned study.

2. If deciding to synchronize animals via egg lay, it is best to do it in two steps. When first getting syncronized day 1 adults (by placing gravid adults for example) and then letting these worms lay eggs - older worms retain eggs and so eggs' age can vary and thus using young adults is important.

We thank the reviewer for their insight and have added that synchronized young adult animals should be used for egg-laying. Also, we have included a note about how old animals may release eggs that are in a more advance developmental stage.

3. The concern about the use of FUdR for proteostasis discussed in paper should be noted in section 3 when its use is described.

We thank the reviewer and have made the requested addition (lines 189-190 in the revised manuscript).

4. Proteostasis collapse in C. elegans has some elements that are gradual, however, its regulation was demonstrated to change within hours (Ref 2 in the manuscript; Labbadia and Morimoto 2015 Mol Cell. 2015 59(4):639-50; Shemesh et al., Aging Cell. 2013 12(5):814-22). This should be noted in the discussion.

We thank the reviewer for their insight and have added the following to the discussion (lines 415-417) and added references:

> "In *C. elegans,* the transcriptional inducibility of multiple forms of stress response rapidly decline within a few hours after the onset of reproduction due to the formation of repressive chromatin marks at stress loci".

5. Lines 413-417 discuss a specific work: daf-2 mutant animals showing increased aggregation but improved proteostasis - relating to Cohen et al Science. 2006 Sep 15;313(5793):1604-10. Moreover, ref 40 discussed here show via RNAi screen that aggregation and toxicity are not correlated.

601 Elmwood Avenue • Box 633 • Rochester, NY 14642
585-273-2409 • 585-273-1450 fax • andrew_samuelson@urmc.rochester.edu

We thank the reviewer for catching our unintended oversight. We apologize and have added references for the Cohen et al. and Silva et. al. studies to this portion of the discussion.

6. There is no ref to FRAP data on protein aggregation, please add citation to refs: 15 and 31 in line 439.

We thank the reviewer for our oversight. We found several additional instances where FRAP was mentioned, but not properly referenced. In the revised manuscript we reference Morley 2002, Brignull 2006, and Garcia 2007 throughout.

7. Also, there are biochemical methods to asses aggregation that can also be used and should be mentioned - Nollen et al., Proc Natl Acad Sci U S A. 2004 101(17):6403-8

We thank the reviewer and have added a line to the discussion and this reference.

8. In line 485 the a problem with the full name of GABA.

We have made the required changes.

601 Elmwood Avenue • Box 633 • Rochester, NY 14642
585-273-2409 • 585-273-1450 fax • andrew_samuelson@urmc.rochester.edu

Supplemental File 1

Click here to access/download;Supplemental File (Figures, Permissions, etc.);Supplemental File 1.xlsx

Com

[1]

[2]

[3]

[1]

[2]

[3]

[1]

[2]

[3]

[4]

[5]

[1]
[2]
[3]
[4]

[1]

[2]

[3]

[4]

[5]

mon reagents- Agar plates for *C. elegans* growth and maintenance

Standard NGM plate recipe (per 1 L):

Add 1 L ultrapure water to a 2 L flask, followed by 17 g agar, 3 g NaCl, and 2.5 g bacto-peptone. Thoroughly mix on a stir plate with a sterilized stir bar, and then autoclave on a program for liquids.

After the autoclave run is complete, resume stirring on the stir plate at a medium speed. Using sterile technique add the following: 1 mL Cholesterol (5 mg/mL), 1 mL 1 M $CaCl_2$, 1 mL 1 M $MgSO_4$, and 25 mL 1 M KPO_4.

When the agar has cooled enough but is still fluid- under 55 °C but higher than 40 °C- add 250 µL nystatin (40 mg/mL) and 8 mL streptomycin (25 mg/mL). After allowing a few minutes for mixing, follow standard lab protocol for pouring plates. 1 L is enough for approximately 80 6 cm plates (12 mL per plate), or 25 10 cm plates (36 mL per plate).

Note: The use of both nystatin and streptomycin is an optional choice to prevent contamination.

RNAi plate recipe (per 1 L):

Add 1 L ultrapure water to a 2 L flask, followed by 17 g agar, 3 g NaCl, and 2.5 g bacto-peptone. Thoroughly mix on a stir plate with a sterilized stir bar, and then autoclave on a program for liquids.

After the autoclave run is complete, resume stirring on the stir plate at a medium speed. Using sterile technique add the following: 1 mL Cholesterol (5 mg/mL), 1 mL 1 M $CaCl_2$, 1 mL 1 M $MgSO_4$, and 25 mL 1 M KPO_4.

When the agar has cooled enough but is still fluid- under 55 °C but higher than 40 °C- add 1 mL carbenicillin (25 mg/mL) and 6 mL 0.2 g/mL IPTG (Isopropyl β-D-1-thiogalactopyranoside). After allowing a few minutes for mixing, follow standard lab protocol for pouring plates. 1 L is enough for approximately 80 6 cm plates (12 mL per plate), 25 10 cm plates (36 mL per plate), or 25 24-well plates (1.5 mL per well).

Common reagents- M9 Buffer Solution

M9 buffer recipe (per 1 L):

Add 0.75 L ultrapure water to a 1 L flask, with a sterile stir bar on a stir plate.

Add the following and allow to dissolve: 3 g monobasic $KH-_2PO_4$, 6 g dibasic Na_2HPO_4, 5 g NaCl.

Add another 0.25 L ultrapure water. Allow to mix.

Distribute to autoclavable bottles of the desired volume. Autoclave on a program for liquids. When completed, remove and allow to cool.

Once cool, add 1 mL per liter of 1M $MgSO_4$ to each bottle.

Common reagents- Hypochlorite Solution

recipe (10 mL):

6.0 mL bleach
3.2 mL 5 N NaOH
0.8 mL MQ H2O
Bleach is light sensitive. Store for up to 2 weeks at RT.

Common reagents- Plates for bacterial culture

LB + ampicillin + tetracycline agar plate recipe (per 1 L):

Add 32 g LB agar to 1 L of ultrapure water with a sterile stir bar in a 2 L flask. Stir on a stir plate.

Once well-mixed, add 1.5 mL 2 N NaOH.
Autoclave on a liquid program. When autoclaving is complete, re-place on stir plate and allow to cool (with stirring) until reaching 55 °C.
Add 3 mL of 5 mg/mL tetracycline, and 1 mL of 50 mg/mL ampicillin. Allow to mix.
Use standard lab plate pouring procedures to dispense about 45 mL sterilized liquid LB agar mix per rectangular plate (Nunc Omnitray non-treated 128x86 mm or similar).

Supplemental Table 1

Click here to access/download;Supplemental File (Figures, Permissions, etc.);Supplemental Table 1.xlsx

Number of foci per animal

Strain: *unc-54p::Q35::YFP*

D1	D2	D3	D4
5	10	31	37
7	25	20	54
4	22	35	57
7	5	22	39
9	15	31	38
11	19	27	46
9	26	21	43
6	14	20	36
10	15	22	48
9	10	39	32
6	17	27	37
4	18	37	37
2	16	40	38
5	12	36	42
7	12	37	49
7	13	24	38
6	18	22	41
9	10	25	44
8	13	28	43
10	13	25	36
6	13	25	38
12	17	19	46
7	15	24	30
8	14	29	38
9	13	21	38
4	13	22	
7	10	34	
	18	34	
	16	31	
	17	30	
	20	30	
	16	24	
		33	
		32	
		20	
		27	
		37	
		33	
		20	

Paralysis rate

Strain: *unc-54p::Q35::YFP*

	D3	D5	D7	D9
Paralyzed animals:	0	1	2	37
Total animals:	54	54	54	54
Rate:	0	0.01851852	0.03703704	0.68518519
SEM	0	0.01852	0.02594	0.0638

Number of foci per animal

Strain: *rgef-1p::Q40::YFP*

D4 NT	D6 NT	D8 NT	D10 NT
4	4	3	5
3	4	8	3
4	3	4	7
3	4	5	5
2	5	7	5
4	4	3	4
3	5	6	3
3	11	6	5
2	5	7	4
0	4	4	5
1	3	11	4
3	8	4	4
1	3	3	6
2	4	5	7
2	4	8	9
2	3	1	7
1	3	5	5
1	5	3	4
2	2	4	10
4	2	8	11
2	5	3	5
4	7	3	4
	3	4	
	4	7	
	4	7	
	3	7	
	5		
	3		

Body bends in 30 sec per animal

Day 2 adult animals

WT	*rgef-1p::Q40::YFP*
47	3
51	10
48	21
46	16
40	8
49	24
44	21
42	26
55	30
44	18
44	8
41	9
40	10
47	10
57	17
42	24
54	2
53	0
53	10
51	14
45	6
45	9
56	9
48	11
50	14
48	5
45	13
49	14
51	8
54	23
55	7
50	16
56	3
53	8
47	20
41	7
51	10
55	
53	